Published in final edited form as:
Brain Res. 2009 November 24; 1299: 33–44. doi:10.1016/j.brainres.2009.07.016.

Intracranial electroencephalography reveals two distinct similarity effects during item recognition

Marieke K. van Vugt[a,*], **Andreas Schulze-Bonhage**[b], **Robert Sekuler**[c], **Brian Litt**[d], **Armin Brandt**[b], **Gordon Baltuch**[e], and **Michael J. Kahana**[f]

[a] Center for the Study of Brain, Mind and Behavior. Green Hall. Princeton University, Princeton, 08540, USA. Phone: 609-258-5032. Fax: 609-258-2549

[b] University Hospital of Freiburg, Freiburg, Germany

[c] Volen Center for Complex Systems, Brandeis University, Waltham, MA

[d] Depts. of Neurology and Bioengineering, University of Pennsylvania, Philadelphia, PA

[e] Dept. of Neurosurgery, University of Pennsylvania, Philadelphia, PA

[f] Dept of Psychology, University of Pennsylvania, Philadelphia, PA

Abstract

Behavioral studies of visual recognition memory indicate that old/new decisions reflect both the similarity of the probe to the studied items (probe–item similarity) and the similarities among the studied items themselves (list homogeneity). Recording intracranial electroencephalography from 1,155 electrodes across 15 patients, we examined the oscillatory correlates of probe–item similarity and homogeneity effects in short-term recognition memory for synthetic faces. Frontal areas show increases in low-frequency oscillations with both probe–item and item–item similarity, whereas temporal lobe areas show distinct oscillatory correlates for probe–item similarity and homogeneity in the gamma band. We discuss these frontal low-frequency effects and the dissociation in the temporal lobe in terms of recent computational models of visual recognition memory.

Keywords

oscillations; recognition memory; cognitive modeling; similarity

1 Introduction

Similarity is an important factor in human forgetting, as interference between items increases when those items are similar within a psychological representational space (Robinson, 1927). Although parametric investigations of similarity effects in recognition have been widely used in the cognitive literature, the neural correlates of similarity remain largely unexplored. Here we examine the neural correlates of two distinct types of similarity effects in recognition memory. The first of these is participants' increased tendency to endorse a test probe when it is similar to one or more list items (e.g., Hintzman, 1988; Lamberts et al., 2003; Nosofsky, 1991; Shiffrin and Steyvers, 1997). The second is participants' decreased tendency to endorse a test probe when the list items are very similar to one another (Kahana and Sekuler, 2002; Nosofsky and Kantner, 2006; Visscher et al., 2007).

*Email address: mkvan@princeton.edu (Marieke K. van Vugt).

In visual item recognition tasks, participants view a short sequence of study items, followed by a probe item. Their task is to indicate whether the probe matches one of the study items. An influential class of cognitive models describing this visual recognition memory process ("summed similarity models") assumes that participants base their recognition decision on the sum of the similarities between the probe and study items' memorial representations (Hintzman, 1988; Kahana and Sekuler, 2002; Lamberts et al., 2003; Nosofsky, 1991; Nosofsky and Kantner, 2006; Shiffrin and Steyvers, 1997). Similarities can be computed when the multidimensional representations of the stimuli are known (as derived, for example, from a multidimensional scaling procedure). Kahana and Sekuler (2002) in their Noisy Exemplar Model (NEMo), extended this basic framework by incorporating item–item similarity (the mean of all pairwise similarities between study items) in the basic model (Kahana and Sekuler, 2002; Sekuler and Kahana, 2008). They found that when the list is homogeneous (i.e., the list items are highly similar to each other), the probability of responding *yes* decreases. Visscher et al. (2007) showed that this was still the case when probe–item similarity was held constant. We will therefore refer to the mean item–item similarity as a "homogeneity correction," which will tend to push the decision in the opposite direction of probe–item similarity (Viswanathan et al., submitted). Including this extra term significantly improved the model's fit to the data.

In this paper, we have two main objectives. First, we want to examine whether oscillatory correlates of probe–item similarity and the homogeneity correction can be found in intracranial electroencephalography (EEG) recordings. Second, we aim to exploit the neural data in a novel way, namely in order to select among alternative models of the recognition process. In particular, we compare the neural correlates of probe–item similarity and the homogeneity correction to see whether the latter is a useful addition of NEMo to summed similarity models.

There are various possible outcomes of such an analysis. We predict that probe–item similarity and the homogeneity correction are associated with *different* neural correlates, since behavioral evidence suggests that they involve distinct computations (Visscher et al., in press). It could, however, also be the case that probe–item similarity and the homogeneity correction are associated with the *same* neural signatures, which could point to generic mechanisms that sum similarity across items. Thirdly, if probe–item similarity and the homogeneity correction have similar neural signatures but are opposite in sign, that would indicate neural processes that are involved in computing the sum of probe–item similarity and the homogeneity correction that forms the basis for the recognition decision (to which probe–item and item–item similarity make opposite contributions). Finally, if the homogeneity correction were to show little or no correlation with neural activity, this would make it a less plausible addition to the summed similarity model. If we do not find any neural correlates of NEMo, this would indicate that oscillatory activity is not the prime locus for visual recognition memory.

Which brain regions would be expected to show correlates of the two similarity signals? There is an extensive literature on the neural correlates of short-term memory for non-verbal stimuli such as faces, which are the stimuli we used in this experiment. For probe–item similarity only, we expected the neural correlates to be similar to differences in neural activity for targets and lures ("old/new effects") that have been reported in the literature. These old/new effects have been found in the left parietal lobe in scalp EEG (e.g., Curran, 2000; Düzel et al., 2005) and functional magnetic resonance imaging (fMRI) studies (e.g., Kahn et al., 2004; Wagner et al., 2005). Furthermore, targets and lures also show differential fMRI blood oxygenation level-dependent (BOLD) activity and potentials in intracranial EEG in the dorsolateral pre-frontal cortex (DLPFC) and the medial temporal lobe (MTL) (Cabeza et al., 2001; Ludowig et al., 2008, respectively). Given that our focus here is on the integration of two similarity signals (probe–item similarity and the homogeneity correction), we also expected to see correlates of both of these signals (probe–item similarity and the homogeneity correction) in the frontopolar cortex (Brodmann area 10). This is a region that has been associated with the integration of

information from multiple sub-tasks (e.g., deciding whether multiple items share the same property) in working memory tasks (Braver and Bonglolatti, 2002; Koechlin et al., 1999; Koechlin and Hyafil, 2007; Ramnani and Owen, 2004; Reynolds et al., 2006). It also shows increased activation with supra-span memory loads and during episodic memory retrieval (Cabeza et al., 1997; Christoff and Gabrieli, 2000).

In addition to judging the plausibility of the model and its neural correlates on their spatial locations, we will examine their location in frequency space. Based on a scalp EEG study (van Vugt et al., submitted), we expect probe–item similarity to correlate with left parietal 4–9 Hz theta oscillations. Oscillations in both the theta (4–9 Hz) and gamma (28–128 Hz) bands have frequently been associated with memory and attentional processes (e.g., Osipova et al., 2006; Rizzuto et al., 2006; Sederberg et al., 2007b). If we fail to find oscillatory correlates in BA 10, parietal areas and the MTL, in frequency bands that include theta and gamma, then oscillatory activity does not play a large role in visual recognition memory.

To study the oscillatory correlates of probe–item similarity and the homogeneity correction we tested participants in a visual Sternberg task (Sternberg, 1966). The stimuli consisted of a set of synthetic male faces (Wilson et al., 2002). The advantages of using this face set are that, although the face stimuli are well-controlled, they still can be identified with high accuracy (Wilson et al., 2002), and it is possible to measure their inter-item similarity precisely. Moreover, the face stimuli are realistic enough to generate strong responses in the fusiform face area (Loffler et al., 2005), and we have previously shown how their similarity structure affects recognition memory performance (van Vugt et al., submitted) and the learning of name–face associations (Pantelis et al., 2008).

Detecting medial temporal lobe activity and separating it from e.g., the medial temporal gyrus requires excellent spatial resolution, beyond that of scalp EEG. For that reason, we used intracranial EEG (iEEG) recordings to study the oscillatory correlates of probe–item similarity and the homogeneity correction. Although we focus our analyses mainly on the above-mentioned regions of interest, we will also use whole-brain analyses to examine the specificity of the effects.

2 Experimental Procedures

We recorded iEEG in 1,155 electrodes from 15 neurosurgical patients (ages 15–58, 6 female, 9 male) being treated for pharmacologically intractable epilepsy. These patients were implanted with arrays of subdural and/or depth electrodes for seizure localization and functional mapping. The clinical team determined the placement of the electrodes with these goals in mind. Our research protocol was approved by the appropriate institutional review boards, and informed consent was obtained from the participants and their guardians. The recordings took place at Brigham and Women's Hospital in Boston, the Hospital of the University of Pennsylvania in Philadelphia, and Universitäts Klinikum Freiburg in Germany.

2.1 Behavioral task

Participants performed a short-term item recognition task (Figure 1). Lists consisted of 1, 2, and 3 faces for which the similarity space has been well-characterized (Pantelis et al., 2008; van Vugt et al., submitted; Wilson et al., 2002).

The faces were designed to vary along the four principal components of a 37-dimensional face space (Wilson et al., 2002). This face space had been created by taking 37 measurements on a set of (normalized) photographs of Caucasian males, and then reconstructing the faces from the principal components that could be extracted from the matrix of these measurements. A stimulus set of 16 faces was created from all permutations of steps of one standard deviation

away from the mean face (of the 37-dimensional face space) in the directions of each of the first four principal components (one standard deviation is approximately the threshold for 75% correct discrimination between two faces that are flashed for 110 ms; see Appendix). To determine the psychological representation of our stimuli, we performed a separate multidimensional scaling (MDS) study, which is described more extensively in Pantelis et al. (2008). Briefly, 23 participants saw all combinations of 3 faces twice, and were requested to identify the "odd-one-out". From these ratings, a similarity matrix was constructed by increasing the similarity value for each of the two non-chosen faces (see Kahana and Bennett, 1994, for details). This similarity matrix was transformed into similarity coordinates for every face using individual differences multidimensional scaling (INDSCAL/ALSCAL; Takane et al., 1977). A four-dimensional solution was chosen, which was a good fit according to an inspection of the scree plot, and also corresponded to the number of dimensions on the basis of which the faces had been generated. The MDS-derived coordinates were then used in the model fitting process.

During the recognition memory trials, the stimuli were constrained such that none could be repeated on two successive lists, with the exception of the lure probes that could have been a study item 1, 2, or 3 lists ago (a "recent negatives" manipulation (Monsell, 1978)). Each trial started with presentation of a fixation cross (1000–1075 ms, jittered). Each list item was then shown for 700–775 ms, with a 275–350 ms inter-stimulus interval. The participant was asked to indicate whether the probe item that appeared after a delay of 3000–3300 ms was or was not a member of the just-presented list (i.e., target or lure), and was given immediate feedback on their accuracy. The participant could then initiate the next trial with a button press. Temporal jitter was employed to avoid spurious correlations between ongoing oscillations and the structure of the task. The experiment was programmed in the freely available Python-based experiment programming library PyEPL (http://pyepl.sourceforge.net; described in in Geller et al., 2007).

We ensured equal probabilities of target and lure items, of the three list lengths, of the three levels of proactive interference (the list lags of the lure probes), and of the three possible item lags of target probes. We created blocks of trials such that each block comprised 15 lists in which there are an equal number of target and lure trials, and each item served as a lure only once. We randomized the order of blocks across participants but kept the list order within blocks fixed, which ensured that every participant saw lists with the same levels of proactive interference. Every session was preceded by two 16-trial training blocks, plus 40 additional one-item lists to familiarize the participant with the face stimuli. Participants were given feedback on their average accuracy and RT at the end of each block. Incorrect trials and trials with RTs shorter than 200 ms or longer than 3500 ms were removed from the analysis.

2.2 iEEG recordings

The iEEG signal was recorded from either subdural grids or depth electrodes, using either a NeuroFile or Nicolet digital recording system (depending on the site). Depending on the amplifier, the signals were sampled at 250, 256, 400, 512, or 1024 Hz, and band-pass filtered between 0.3 and 70 Hz or 0.1 and 100 Hz. Data were subsequently notch-filtered with a Butterworth filter with zero phase distortion between 48 and 52 Hz or 58 and 62 Hz to eliminate the relevant line noise. Intervals of interest in the EEG signal were scanned for artifacts by means of a kurtosis threshold; events were discarded if its kurtosis exceeded a threshold of 5 (Delorme and Makeig, 2004).

To synchronize the electrophysiological recordings with behavioral events, the experimental computer sent pulses through the parallel or USB port via an optical isolator into an unused recording channel or digital input on the amplifier. The time stamps associated with these pulses aligned the experimental computer's clock with the iEEG clock to a precision well under the

sampling interval of the iEEG recording (< 4 ms). For all participants, the locations of the electrodes were determined by means of co-registered post-operative CTs and pre-operative MRIs, or from post-operative MRIs, by an indirect stereotactic technique, and converted into Talairach coordinates.

2.3 Data analysis

After resampling the data to 256 Hz, we used the Morlet wavelet transform with a wave number of 6 to compute spectral power as a function of time for the EEG signals of interest (Tallon-Baudry et al., 1997; van Vugt et al., 2007). For each trial, the time window of interest extended from 1000 ms before probe onset, until 2000 ms after the probe. The first and last second of this interval only served as a buffer to avoid edge artifacts and were subsequently discarded. For every frequency, we z-transformed the data to the mean and standard deviation of the power during the 1000-ms fixation interval. This normalizes any drift that may be in the data and ameliorates the low-frequency bias (Freeman, 2006). We assumed that the effects of interest took place at a 100-ms timescale, and therefore calculated the average oscillatory power within each 100-ms time interval.

For the analysis of the retrieval interval we utilized a multiple regression approach to predict the influence of multiple interference variables simultaneously (Jacobs et al., 2006; van Vugt et al., submitted). This model was applied separately to every electrode, time interval, and frequency, after which the maximum regression coefficient was taken within each frequency band. We then asked whether the regression coefficients of the electrodes within any particular Brodmann area (defined by the Talairach Daemon, Lancaster et al. (2000)) significantly differed from zero. This hypothesis was tested with a Wilcoxon signed rank test. Final significance was determined using a *p*-value threshold set by a False Discovery Rate (FDR) procedure (Benjamini and Hochberg, 1995). A FDR of 0.01, which is the threshold we used, means that on average 1% of the significant electrodes across all frequency bands and time intervals could be false positives. Note that this differs from conventional *p*-value testing, where a *p*-value of 0.05 indicates that on average 5% of cases that in fact do not reject the null hypothesis will be called significant. In our study, a FDR of 0.01 corresponded to a *p*-value threshold of 1.4*10–4. Only Brodmann areas with a minimum of 10 electrodes and 4 contributing participants were included in the analyses.

To examine whether the regression coefficients differed between regions and similarity type (probe–item similarity, item–item similarity/homogeneity correction), we applied a multi-way ANOVA on the regression coefficients with the factors frequency band, time interval (early (0–500 ms) vs late (500–1000 ms)), Brodmann area, and similarity effect (probe–item or item–item). The number of time bins was reduced to 2, because an inspection of the time course of the results revealed that the effect is on the order of 500 ms. This reduction in time bins us to simplify the analysis. For the region of interest analysis, we then separately plotted the time courses for each of the regions of interest (i.e., frontal and memory regions). To visualize the whole-brain analyses, we overlaid the Brodmann areas defined by the Talairach Daemon on the standard MNI brain by using information in the WFU PickAtlas toolbox (Maldjian et al., 2003).

3 Results

The Noisy Exemplar Model (Kahana and Sekuler, 2002) assumes that participants base their recognition decision largely on the summed pairwise similarity between an item's memorial representation and the representation of the test probe. Formally, this probe–item similarity is given by:

$$S = \sum_{i=1}^{L} \alpha_i e^{-\tau|\mathbf{s_i}-\mathbf{p}|} \tag{1}$$

Here L refers to the length of the study list, α_i is a forgetting parameter as described below, τ determines the form of the exponential generalization gradient (Shepard, 1987), $\mathbf{s_i}$ is the vector representing the coordinates of the memorial representation of stimulus i, and $\mathbf{p}$ is the representation of the probe item. The summed similarity of a target probe to the members of the study list typically exceeds the summed similarity of lure probes to the members of the study list. NEMo extends the basic summed similarity framework for item recognition (Hintzman, 1988; Nosofsky, 1991) by showing that the degree of summed similarity required to respond *yes* varies with list homogeneity (i.e., the mean similarity among list items). With greater list homogeneity, participants will respond *yes* at lower levels of summed similarity (Kahana et al., 2007; Nosofsky and Kantner, 2006; Visscher et al., 2007). Formally, homogeneity is defined as the average similarity among the L studied items:

$$H = \frac{2\beta}{L(L-1)} \sum_{i=1}^{L-1} \sum_{j=i+1}^{L} e^{-\tau|\mathbf{s_i}-\mathbf{s_j}|} \tag{2}$$

In this equation, β determines the influence of list homogeneity. According to NEMo, the probability of responding *yes* is given by:

$$P(yes) = P(S + H > c_L) \tag{3}$$

Here c_L is a separate decision criterion for every list length. Each item's memorial representation, $\mathbf{s_i}$, is defined by summing the coordinates obtained from an MDS study (Pantelis et al., 2008; van Vugt et al., submitted) with a noise vector whose components are zero-mean Gaussians whose standard deviation (σ) depends on the stimulus dimensions comprising that item. In using this noise term, we can adopt a fully deterministic decision rule (Ashby and Maddox, 1998). Variability in participant's responses from one occurrence to another are modeled by the sampling of each item from the distribution of its noisy representation $\mathbf{s_i}$. To simulate forgetting, NEMo assumes that the most recent stimulus contributes the most to the summed similarity, and that earlier items contribute less and less. This is simulated by the parameter α, which increases with lag ($i = 1$ indicating the most recently studied item). Finally, NEMo allows for the possibility that participants differentially weight the contributions of different stimulus dimensions. These weights, which are not shown in Equation (1), also insure that the measured distances are not sensitive to absolute variations in the scale of the dimensions.

The model parameters were estimated by using a genetic algorithm (Mitchell, 1996) to minimize the root-mean-square deviation (RMSD) between the observed and predicted binned accuracy for each participant. Simulated participants respond *yes* when $S + H > c_L$. The genetic algorithm was run for 20 generations of 2000 individuals each. The obtained estimates of the best-fitting parameters (Table 1) are similar to those reported in previous applications of NEMo (Kahana and Sekuler, 2002; Kahana et al., 2007; Nosofsky and Kantner, 2006; van Vugt et al., submitted; Visscher et al., 2007; Yotsumoto et al., 2007). In particular, the parameter β is significantly smaller than zero [$t(14) = -11.7$, $p < 0.001$]. This indicates that list homogeneity contributes significantly to the old/new decision.

Oscillatory correlates of probe–item and item–item similarity

Our main research question was whether probe–item similarity and the homogeneity correction have distinct neural correlates and whether these neural correlates support NEMO. To investigate the oscillatory correlates of these two variables simultaneously, we used a regression model, which we have introduced in previous scalp EEG studies (Jacobs et al., 2006; van Vugt et al., submitted). We regressed oscillatory power on three factors: summed probe–item similarity (*S*), mean inter-item similarity (homogeneity, *H*), and lag (*lag*):

$$\text{Targets model: } P_{freq,electrode,time} = \beta_0 + \beta_1 S + \beta_2 H + \beta_3 lag_T + \varepsilon \quad (4)$$

$$\text{Lures model: } P_{freq,electrode,time} = \beta_0 + \beta_1 S + \beta_2 H + \beta_3 lag_L + \varepsilon \quad (5)$$

In these regression models, the Lag variable measures how recently a probe item has been last studied, either on the current list (for targets) or on a previously studied list (for lures). This variable was included to statistically remove recency and proactive interference effects (e.g., McElree and Dosher, 1989; Monsell, 1978). Since recency and proactive-interference were not a focus of the present study, we will not discuss oscillatory correlates of the lag variable here.

We computed these regressions separately for each electrode, frequency-band, and each of ten successive 100-ms time intervals following probe onset. To avoid confounding the oscillatory correlates of probe–item similarity with well known old–new effects (Düzel et al., 2003), we fit separate regression models to data for targets and lures. The regression coefficients were combined in Brodmann areas as described in the Experimental Procedures (see also Sederberg et al. (2007a)). The results are presented in tabular format, in which a positive or negative sign indicates a significantly positive or negative correlation between oscillatory activity and *S* or *H* in at least one of the 10 time bins. The number of participants contributing electrodes to each region are shown in the last two columns of each table. Note that this table shows 18 significant results, of which 0.18 on average (i.e., 1%) are spurious according to the FDR procedure.

We will discuss each of the regions of interest in turn: first the frontopolar cortex, which, because of its role in information integration (e.g., Ramnani and Owen, 2004), should show correlates of both *S* and *H*. After that, we will discuss the DLPFC, the left parietal lobe, and lastly temporal regions. The results are presented in Table 2.

In Brodmann area (BA) 10 (the frontopolar cortex), 2–4 Hz delta oscillations increase with both *S* and *H* for targets. For lures, 9–14 Hz alpha oscillatory power decreases and increases with *S* and *H*, respectively. Additionally, 90–128 Hz gamma oscillatory power is positively and negatively correlated with *S* for lures and targets, respectively. Note that this effect could reflect task difficulty because higher probe–item similarity (*S*) is more difficult for lures and easier for targets.

In addition to the low-frequency integration signals in the frontopolar cortex, we found similar effects in the DLPFC. In right BA 46 (part of the DLPFC), 2–4 Hz delta oscillatory power increases both with *S* and *H*. Another region in the DLPFC, BA 9 (DLPFC) shows a decrease in 28–48 Hz gamma power with *S*, which might again reflect difficulty.

Furthermore, we expected to see correlates of *S* in the left parietal lobe, a region that has frequently been found to show old/new effects. These are notably absent. This might in large

part be related to the fact that there are relatively few electrodes in the left hemisphere (see Table 2).

The last regions of interest are those in the temporal lobe. These memory-related areas show different effects for *S* and *H*. In the left medial temporal gyrus (MTG; BA 21), a brain region that was previously shown to exhibit subsequent memory effects in the gamma band (Sederberg et al., 2007b), 24–48 Hz gamma oscillatory power decreases with *S*. In the right superior temporal gyrus (STG; BA 22) on the other hand, 14–28 Hz beta and 90–128 Hz gamma power increase with *S*. These regions on the temporal gyrus do not show a significant correlation with *H*. This is in contrast with deeper temporal regions, where alpha power in the right entorhinal cortex and left hippocampus increase with *H* and there is no significant effect of *S*.

To formally test the interaction between similarity effect and brain region/frequency, we performed a similarity type (*S*, *H*) by region (hippocampus, entorhinal, BA 21, BA 22) by time-bin (early, 0–500 ms; late, 500–1000 ms) by frequency band ANOVA. This analysis revealed significant main effects of similarity type [F (1, 7112) = 9.78, $p < 0.01$], region [F (3, 7112) = 11.67, $p < 0.001$], and frequency [F (6, 7112) = 21.52, $p < 0.001$]. Crucially, there is also an interaction between similarity type and region [F (3, 7112) = 9.68, $p < 0.001$]. This interaction indicates that the temporal gyrus areas has larger regression coefficients for *S*, and the MTL areas (hippocampus and entorhinal cortex) have larger regression coefficients for *H*.

We then performed a whole-brain analysis to check the specificity of the effects. The Appendix shows that in addition to the above-mentioned regions of interest, there are significant similarity effects in BA 4/6, the (pre-)motor cortex. This Brodmann area shows (for targets) an increase of 4–9 Hz theta oscillatory power with *S*, but a decrease with *H* (Table 2). For lures, 9–14 Hz alpha power increases with probe–item similarity. This comports well with behavioral findings of Kahana and Sekuler (2002) and Nosofsky and Kantner (2006), which show that probe–item similarity and the homogeneity correction are summed with opposite signs, such that they push the *yes/no* decision in opposite directions.

4 Discussion

We demonstrated that correlations can be found between oscillatory brain activity and two theoretical constructs: probe–item similarity and the homogeneity correction. The homogeneity correction is a relatively recent addition to the summed similarity framework, and our finding of neural correlates provides further support for its addition. For oscillatory activity to show clear involvement in visual recognition memory, we required three parts of the brain–BA 10, left parietal lobe and the MTL–to show significant correlations with the model. We found neural correlates of NEMo in two of these three areas. In BA 10, oscillatory gamma power decreased with *S* for targets and increased with *S* for lures. In the temporal lobe, we found in fact a dissociation between *S* and *H*, where *S* was related to gamma oscillatory power in the temporal gyrus, and *H* to alpha oscillatory power in the entorhinal cortex and hippocampus. This suggests that probe–item similarity and the homogeneity correction are indeed two different neural processes. Not anticipated was an increase of 4–9 Hz theta oscillatory power with *S* and a decrease with *H* in the motor cortex (BA 4/6), although, as we will elaborate on, this could be expected based on the perceptual decision making literature. We will now discuss the caveats of the study, followed by the implications of each of our main findings in turn.

The relation between probe–item similarity and the homogeneity correction

First, one might worry that *S* and *H* are not completely independent, which might lead to collinearity issues in the regression analysis. Although their correlation is fairly weak ($r = -0.12$ on average across participants). This correlation is stronger for targets ($r = -0.40$) than

for lures ($r = 0.01$). One can easily intuit that by realizing that when probe–item similarity is high, necessarily many of the list items reside close together in similarity space. In addition to the weak correlation of *S* and *H* themselves, their neural correlates also do not show evidence for a strong correlation, given that the effects in Table 2 sometimes go in the same direction for *S* and *H*, and sometimes in opposite directions. Nevertheless, it is helpful to keep in mind that there may be some instability in the obtained regression coefficients, due to the small correlation between *S* and *H*. Although there is a potential instability in the individual-subject regression coefficients, the effect on the overall results is small because we use an across-subjects analysis where individual-subject noise will cancel out.

Similarity between neural correlates for targets and lures

On the basis of NEMo and other summed-similarity models, we expected to find similar neural correlates of *S* for targets and lures. A potential explanation for the differences between target and lure effects reported in Table 2 is that the neural populations that correlate with components of summed similarity do not show enough variance in their similarity-related responses for both targets and lures to be detected, since summed similarity is known to vary less for the target population than for the lure population (Sekuler and Kahana, 2008). Another possibility is that *S* has different effects on targets and lures, contrary to the assumptions of NEMo and other summed similarity models.

Alpha oscillations—In the literature on oscillations in the hippocampus and entorhinal cortex, the most prominent frequency is theta (4–9 Hz) (Buzsáki, 2002). In our study, we reported changes in the slightly higher-frequency alpha oscillations with summed similarity. Although previous literature focuses mostly on theta activity, recently oscillations in the alpha frequency have also been related to spatial learning (DeCoteau et al., 2007) and environment familiarity (Nerad and Bilkey, 2005) in rats. In addition, it is important to note that in the animal spatial navigation literature, in many cases theta band activity is defined up to about 13 Hz, which is what we refer to as alpha activity in the current study. In human spatial learning too, prominent alpha activity is found in the MTL (Ekstrom et al., 2005). We propose that learning in humans too might not be restricted to the theta band, although this frequency band has been emphasized in the previous literature (e.g., Kahana et al., 2001; Sederberg et al., 2003).

Role of frontopolar cortex in visual recognition memory—Earlier, we suggested that failure to find a correlate of NEMo in the frontopolar cortex would cast doubts on the neural correlates of the model, because this brain area has been implicated in integrating information in memory tasks. Integrating information is a crucial component in computing the sum of the similarities between two items. In our analysis we found that delta and theta oscillations in the frontopolar cortex (BA 10) increased with both *S* and *H*. This finding comports well with neuroimaging studies that have shown the frontopolar cortex to be important for sub-goal processing during working memory tasks (Braver and Bonglolatti, 2002), and to working memory updating (Van der Linden et al., 1999). The sub-goal in this context of the decision-making process is the summing of the similarities of items. A recent study found activation of the left frontopolar cortex when determining the similarity between word pairs (Green et al., 2006). The right-hemisphere lateralization in our study, using non-verbalizable faces, is in agreement with findings that show right-hemisphere working memory processing for nonverbal stimuli and left-hemisphere processing for verbal stimuli (e.g., Kelley et al., 1998).

We propose that in the frontopolar cortex, a sum is computed of the similarities between the probe and list items, and among the list items themselves. In order to add these two factors into the decision making process, the sign of the inter–item similarity term will need to be inverted, because this factor pushes the recognition decision in the opposite direction of probe–item

similarity. We propose that this happens in a different brain area. For this proposal to hold, *S* and *H* should correlate with different sub-populations of cells within the frontopolar cortex.

Another region that shows this low-frequency effect is BA 46 in the DLPFC. Previous studies have found that BA 46 is very important in perceptual decision-making (Heekeren et al., 2008), where it has been proposed to aggregate the accumulated sensory information to come to a perceptual decision. In addition, it shows differential activity for targets and lures (e.g., Cabeza et al., 2001). We propose that in this case BA 46 works together with the frontopolar cortex to sum the similarities of study items to each other and to the probe. It would be interesting to apply accumulator models of recognition memory (e.g., Lamberts et al., 2003; Nosofsky and Palmeri, 1997) to these data, and to examine their neural correlates to strengthen evidence for this proposal.

Dissociation in temporal regions between probe–item and item–item similarity—*S* was associated with gamma oscillations in the left medial temporal gyrus (MTG) and right superior temporal gyrus (STG), whereas *H* was associated with an increase in alpha oscillations in the right entorhinal cortex and left hippocampus. This might be analogous to a finding by Konishi et al. (2006), who found that encoding of isolated items in a word list was associated with more lateral temporal activation, whereas encoding of words focusing on the relations between items led to more hippocampal involvement. In our study, the dissociation between the two similarity effects in brain regions and frequency could reflect the fact that in computing *S* one needs to combine currently available information (the probe) with retrieved information from episodic memory (the more distant list items). Therefore, in the case of *H*, the focus is on relations between items in the study list, whereas for *S*, there is a larger focus on the probe item. Binding probe and item information requires rehearsal mechanisms and episodic memory, both of which have been associated with the right STG (Klingberg et al., 1996; Osaka et al., 2003) and the left MTG (Elliott and Dolan, 1998). Moreover, the right STG has also been associated with distinguishing probes from similar lures (Kensinger and Schacter, 2007). *H*, in contrast, almost only uses retrieved list item information, and hence it will recruit more strongly structures that are involved in episodic memory (Buckmaster et al., 2004).

Another possibility is that *H* is mainly computed during the list presentation, instead of during probe presentation. In terms used to describe algorithms in computer science, these could be called the eager and lazy strategies (e.g., Aha, 1997). It will be important to examine at what time *H* is computed, because in the previous literature the eager approach has been implicitly assumed but never tested. In fact, it could well be that the neural correlates of *H* reported here are only the tip of the iceberg, and that much stronger effects are present during list presentation.

Similarity effects in motor regions—The motor regions were not among our *a priori* regions of interest. Nevertheless, we found an increase in 4–9 Hz theta oscillatory power with *S* in the motor cortices, and a decrease with *H*. A closer examination of the literature reveals that this is not implausible. BA 4/6 has often been reported to be activated in visual and spatial working memory (e.g., Garavan et al., 2000; Postle and Hamidi, 2007; Rypma et al., 1999; Stern et al., 2000). Moreover, it has recently been suggested that “the human motor system also has an important role in perceptual decision making” (Heekeren et al., 2008). Our finding of a positive relation between theta oscillations and *S*, and a decrease with *H* is exactly what one would expect if the motor cortex implements a lowering of the decision threshold (which is the homogeneity correction) as part of the decision making process (Nosofsky and Kantner, 2006; Viswanathan et al., submitted). If the mean inter–item similarity is high, then a smaller level of probe–item similarity is required to evoke a *yes* response than when inter–item similarity is low (Kahana and Sekuler, 2002; Nosofsky and Kantner, 2006; Visscher et al., 2007; Viswanathan et al., submitted). The localization of this effect in theta oscillations

comports well with the finding of Raghavachari et al. (2001) that theta oscillations gate the Sternberg (1966) task.

In summary, we have shown that neural correlates of NEMo can be found, and these occur mostly in the expected brain regions and frequency ranges. This indicates that oscillatory activity plays a large role in visual item recognition. The main correlates of probe–item similarity (*S*) and the homogeneity correction (*H*) were found in the frontal lobe and MTL. Whereas the frontal areas show generally similar increases in low-frequency activity for *S* and *H*, the correlates for the two similarity signals are distinct in memory-related areas. In these memory-related regions, *S* is related to gamma oscillations in the superior and medial temporal gyrus, and *H* is related to increases in alpha oscillations in the entorhinal cortex and hippocampus. *S* and *H* are correlated in opposite directions with theta oscillations in the (pre-) motor cortex, in agreement with their relation in NEMo. Together, these findings provide further support for the idea of adding *H* to summed similarity models of recognition memory, as was proposed by Kahana & Sekuler in their NEMo model.

A Whole-brain analyses

In Figures A.1 and A.2 we report the oscillatory correlates of probe–item similarity and the homogeneity correction for targets and lures, respectively. Black regions indicate those Brodmann areas that we excluded from our analyses because they contain data from fewer than 4 participants and 10 electrodes. Blue and red regions show significant decreases and increases of oscillatory power with the regressor, respectively.

Acknowledgments

The authors acknowledge support from the CELEST grant SBE 0354378, Conte center grant P50 MH062196 and NIH grants RO1 MH061975, MH068404, EY002158 and MH055678. Further support was provided by the Deutsche Forschungsgemeinschaft (SFB 780, Synaptic Mechanisms, TPC3). The authors would like to thank Josh Jacobs, Sean Polyn, and Christoph Weidemann for helpful discussions and suggestions.

References

Aha DW. Editorial. Artificial Intelligence Review 1997;11 (1–5):7–10.

Ashby, FG.; Maddox, WT. Stimulus categorization. In: Marley, AAJ., editor. Choice, decision, and measurement: Essays in honor of R. Duncan Luce. Lawrence Erlbaum and Associates; Mahwah, NJ: 1998. p. 251-301.

Benjamini Y, Hochberg Y. Controlling the False Discovery Rate: a practical and powerful approach to multiple testing. Journal of Royal Statistical Society, Series B 1995;57:289–300.

Braver TS, Bonglolatti SR. The role of frontopolar cortex in subgoal processing during working memory. NeuroImage 2002;15 (3):523–536. [PubMed: 11848695]

Buckmaster C, Eichenbaum H, Amaral D, Suzuki W, Rapp P. Entorhinal Cortex Lesions Disrupt the Relational Organization of Memory in Monkeys. Journal of Neuroscience 2004;24 (44):9811–9825. [PubMed: 15525766]

Buzsáki G. Theta oscillations in the hippocampus. Neuron 2002;33 (3):325–340. [PubMed: 11832222]

Cabeza R, Mangels J, Nyberg L, Habib R, Houle S, McIntosh AR, Tulving E. Brain regions differentially involved in remembering what and when: a PET study. Neuron 1997;19 (4):863–870. [PubMed: 9354332]

Cabeza, R.; Rao, SM.; Wagner, AD.; Mayer, AR.; Schacter, DL. Can medial temporal lobe regions distinguish true from false? An event-related functional MRI study of veridical and illusory recognition memory; Proc Natl Acad Sci U S A. Apr. 2001 p. 4805-4810.URL http://dx.doi.org/10.1073/pnas.081082698

Christoff K, Gabrieli JDE. The frontopolar cortex and human cognition: evidence for a rostrocaudal hierarchical organization within the human prefrontal cortex. Psychobiology 2000;28 (2):168–186.

Curran T. Brain potentials of recollection and familiarity. Memory & Cognition 2000;28:923–938.

DeCoteau WE, Thorn C, Gibson DJ, Courtemanche R, Mitra P, Kubota Y, Graybriel AM. Learning-related coordination of striatal and hippocampal theta rhythms during acquisition of a procedural maze task. PNAS 2007;104 (13):5644–5649. [PubMed: 17372196]

Delorme A, Makeig S. EEGLAB: an open source toolbox for analysis of single-trial EEG dynamics. Journal of Neuroscience Methods 2004;134:9–21. [PubMed: 15102499]

Düzel E, Habib R, Scott B, Schoenfeld A, Lobaugh N, McIntosh AR, Scholz M, Heinze HJ. A multivariate spatiotemporal analysis of electromagnetic time-frequency data of recognition memory. NeuroImage 2003;18 (2):185–197. [PubMed: 12595175]

Düzel E, Neufang M, Heinze HJ. The oscillatory dynamics of recognition memory and its relationship to event-related responses. Cerebral Cortex 2005;15 (12):1992–2002. [PubMed: 15772372]

Ekstrom AD, Caplan J, Ho E, Shattuck K, Fried I, Kahana M. Human hippocampal theta activity during virtual navigation. Hippocampus 2005;15:881–889. [PubMed: 16114040]

Elliott R, Dolan RJ. The neural response in short-term visual recognition memory for perceptual conjunctions. NeuroImage 1998;7 (1):14–22. [PubMed: 9500834]

Freeman WJ. Origin, structure, and role of background EEG activity. Part 4: Neural frame simulation. Clinical Neurophysiology 2006;117 (3):572–589. [PubMed: 16442345]

Garavan H, Kelley D, Rosen AC, Rao SM, Stein EA. Practice-related functional activation changes in a working memory task. Microscopy Research and Technique 2000;51:54–63. [PubMed: 11002353]

Geller AS, Schleifer IK, Sederberg PB, Jacobs J, Kahana MJ. PyEPL: A cross-platform experiment-programming library. Behavior Research Methods 2007;39(4)

Green AE, Fugelsang JA, Kraemer DJM, Shamosh NA, Dunbar KN. Frontopolar cortex mediates abstract integration in analogy. Brain Research 2006;1096 (1):125–137. [PubMed: 16750818]

Heekeren HA, Marrett S, Ungerleider LG. The neural systems that mediate human perceptual decision making. Nature Reviews Neuroscience 2008;9:467–479.

Hintzman DL. Judgments of frequency and recognition memory in multiple-trace memory model. Psychological Review 1988;95:528–551.

Jacobs J, Hwang G, Curran T, Kahana MJ. EEG oscillations and recognition memory: Theta correlates of memory retrieval and decision making. NeuroImage 2006;15 (2):978–87. [PubMed: 16843012]

Kahana MJ, Bennett PJ. Classification and perceived similarity of compound gratings that differ in relative spatial phase. Perception & Psychophysics 1994;55:642–656. [PubMed: 8058452]

Kahana MJ, Seelig D, Madsen JR. Theta returns. Current Opinion in Neurobiology 2001;11:739–744. [PubMed: 11741027]

Kahana MJ, Sekuler R. Recognizing spatial patterns: A noisy exemplar approach. Vision Research 2002;42:2177–2192. [PubMed: 12207978]

Kahana MJ, Zhou F, Geller AS, Sekuler R. Lure-similarity affects visual episodic recognition: Detailed tests of a noisy examplar model. Memory & Cognition 2007;35:1222–1232.

Kahn, I.; Davachi, L.; Wagner, AD. Functional-neuroanatomic correlates of recollection: implications for models of recognition memory; Journal of Neuroscience. Apr. 2004 p. 4172-4180.URL http://dx.doi.org/10.1523/JNEUROSCI.0624-04.2004

Kelley WM, Miezin FM, McDermott KB, Buckner RL, Raichle ME, Cohen NJ, Ollinger JM, Akbudak E, Conturo TE, Snyder AZEPS. Hemispheric specialization in human dorsal frontal cortex and medial temporal lobe for verbal and nonverbal memory coding. Neuron 1998;20:927–936. [PubMed: 9620697]

Kensinger EA, Schacter DL. Remembering the specific visual details of presented objects: Neuroimaging evidence for effects of emotion. Neuropsychologia 2007;45 (13):2951–2962. [PubMed: 17631361]

Klingberg T, Kawashima R, Roland PE. Activation of multi-model cortical areas underlies short-term memory. European Journal of Neuroscience 1996;8 (9):1965–1971. [PubMed: 8921287]

Koechlin E, Basso G, Pietrini P, Panzer S, Grafman J. The role of the anterior prefrontal cortex in human cognition. Nature 1999;399 (6732):148–151. [PubMed: 10335843]

Koechlin E, Hyafil A. Anterior prefrontal function and the limits of human decision-making. Science 2007;318 (5850):594 –598. [PubMed: 17962551]

Konishi S, Asari T, Jimura K, Chikazoe J, Miyashita Y. Activation shift from medial to lateral temporal cortex associated with recency judgements following impoverished encoding. Cerebral Cortex 2006;16 (4):469–474. [PubMed: 15987880]

Lamberts K, Brockdorff N, Heit E. Feature-sampling and random-walk models of individual-stimulus recognition. Journal of Experimental Psychology: General 2003;132:351–378. [PubMed: 13678373]

Lancaster JL, Woldorff MG, Parsons LM, Liotti M, Freitas CS, Rainey L, Kochunov PV, Nickerson D, Mikiten SA, Fox PT. Automated Talairach atlas labels for functional brain mapping. Hum Brain Mapp Jul;2000 10 (3):120–131. [PubMed: 10912591]

Loffler G, Yourganov G, Wilkinson F, Wilson HR. fMRI evidence for the neural representation of faces. Nature Neuroscience 2005;8 (10):1386–1390.

Ludowig E, Trautner P, Kurthen M, Schaller C, Bien CG, Elger CE, Rosburg T. Intracranially recorded memory-related potentials reveal higher posterior than anterior hippocampal involvement in verbal encoding and retrieval. Journal of Cognitive Neuroscience 2008;20 (5):841–851. [PubMed: 18201126]

Maldjian JA, Laurienti PJ, Kraft RA, Burdette JH. An automated method for neuroanatomic and cytoarchitectonic atlas-based interrogation of fMRI data sets. Neuroimage Jul;2003 19 (3):1233–1239. [PubMed: 12880848]

McElree B, Dosher BA. Serial position and set size in short-term memory: The time course of recognition. Journal of Experimental Psychology: General 1989;118:346–373.

Mitchell, M. An introduction to Genetic Algorithms. MIT Press; Cambridge, MA: 1996.

Monsell S. Recency, immediate recognition memory, and reaction time. Cognitive Psychology 1978;10:465–501.

Nerad L, Bilkey DK. Ten- to 12-hz EEG oscillation in the rat hippocampus and rhinal cortex that is modulated by environmental familiarity. Journal of Neurophysiology 2005;93:1246–1254. [PubMed: 15738273]

Nosofsky RM. Tests of an exemplar model for relating perceptual classification and recognition memory. Journal of Experimental Psychology: Human Perception and Performance 1991;17 (1):3–27. [PubMed: 1826320]

Nosofsky RM, Kantner J. Exemplar similarity, study list homogeneity, and short-term perceptual recognition. Memory and Cognition 2006;34 (1):112–124.

Nosofsky RM, Palmeri TJ. An exemplar-based random walk model of speeded classification. Psychological Review 1997;104:266–300. [PubMed: 9127583]

Osaka M, Osaka N, Kondo H, Morishita M, Fukuyama H, Aso T, Shibasaki H. The neural basis of individual differences in working memory capacity: an fMRI study. NeuroImage 2003;18 (3):789–797. [PubMed: 12667855]

Osipova, D.; Takashima, A.; Oostenveld, R.; Fernndez, G.; Maris, E.; Jensen, O. Theta and gamma oscillations predict encoding and retrieval of declarative memory; J Neurosci. Jul. 2006 p. 7523-7531.URL http://dx.doi.org/10.1523/JNEUROSCI.1948-06.2006

Pantelis PC, van Vugt MK, Sekuler R, Wilson HR, Kahana MJ. Why are some people's names easier to learn than others? The effects of similarity on memory for face-name associations. Memory & Cognition 2008;36 (6):1182–1195.

Postle BR, Hamidi M. Nonvisual codes and nonvisual brain areas support visual working memory. Cerebral Cortex 2007;17:2151–2162. [PubMed: 17150984]

Raghavachari S, Rizzuto DS, Caplan JB, Kirschen MP, Bourgeois B, Madsen JR, Kahana MJ, Lisman JE. Gating of human theta oscillations by a working memory task. Journal of Neuroscience 2001;21:3175–3183. [PubMed: 11312302]

Ramnani N, Owen AM. Anterior prefrontal cortex: insights into function from anatomy and neuroimaging. Nature Reviews Neuroscience 2004;5:184–194.

Reynolds JR, McDermott KB, Braver TS. A direct comparison of anterior prefrontal cortex involvement in episodic retrieval and integration. Cerebral Cortex 2006;16 (4):519–528. [PubMed: 16049191]

Rizzuto DS, Madsen JR, Bromfield EB, Schulze-Bonhage A, Kahana MJ. Human neocortical oscillations exhibit theta phase differences between encoding and retrieval. NeuroImage 2006;31 (3):1352–1358. [PubMed: 16542856]

Robinson ES. The 'similarity' factor in retroaction. American Journal of Psychology 1927;39 (14):297–312.

Rypma B, Prabhakaran V, Desmond JE, Glover GH, Gabrieli JDE. Load-dependent roles of frontal brain regions in the maintenance of working memory. NeuroImage 1999;9:216–226. [PubMed: 9927550]

Sederberg PB, Kahana MJ, Howard MW, Donner EJ, Madsen JR. Theta and gamma oscillations during encoding predict subsequent recall. Journal of Neuroscience 2003;23 (34):10809–10814. [PubMed: 14645473]

Sederberg PB, Schulze-Bonhage A, Madsen JR, Bromfield EB, Litt B, Brandt A, Kahana MJ. Gamma oscillations distinguish true from false memories. Psychological Science 2007a;18 (11):927–932. [PubMed: 17958703]

Sederberg PB, Schulze-Bonhage A, Madsen JR, Bromfield EB, Mc-Carthy DC, Brandt A, Tully MS, Kahana MJ. Hippocampal and neocortical gamma oscillations predict memory formation in humans. Cerebral Cortex 2007b;17 (5):1190–1196. [PubMed: 16831858]

Sekuler R, Kahana MJ. A stimulus-oriented approach to memory. Current Directions in Psychological Science 2008;16:305–310.

Shepard RN. Toward a universal law of generalization for psychological science. Science 1987;237:1317–1323. [PubMed: 3629243]

Shiffrin RM, Steyvers M. A model for recognition memory: REM—retrieving effectively from memory. Psychonomic Bulletin and Review 1997;4:145.

Stern CE, Owen AM, Tracey I, Look RB, Rosen BR, Petrides M. Activity in ventrolateral and mid-dorsolateral prefrontal cortex during nonspatial visual working memory processing: Evidence from functional magnetic resonance imaging. NeuroImage 2000;11:392–399. [PubMed: 10806026]

Sternberg S. High-speed scanning in human memory. Science 1966;153:652–654. [PubMed: 5939936]

Takane Y, Young FW, de Leeuw J. Nonmetric individual differences multidimensional scaling: an alternating least squares method with optimal scaling features. Psychometrika 1977;42 (1):7–67.

Tallon-Baudry C, Bertrand O, Delpuech C, Permier J. Oscillatory gamma-band (30–70 hz) activity induced by a visual search task in humans. Journal of Neuroscience 1997;17 (2):722–34. [PubMed: 8987794]

Van der Linden, M.; Collette, F.; Salmon, E.; Delfiore, G.; Degueldre, C.; Luxen, A.; Franck, G. The neural correlates of updating information in verbal working memory. Psychology Press; New York, USA, Ch: 1999. Neuroimaging and Memory; p. 549-560.

van Vugt MK, Sederberg PB, Kahana MJ. Comparison of spectral analysis methods for characterizing brain oscillations. Journal of Neuroscience Methods 2007;162 (1–2):49–63. [PubMed: 17292478]

van Vugt MK, Sekuler R, Wilson HR, Kahana MJ. Distinct electrophysiological correlates of proactive and similarity-based interference in visual working memory. submitted

Visscher KM, Kahana MJ, Sekuler R. Trial-to-trial carryover in auditory short-term memory. Journal of Experimental Psychology: Learning, Memory, and Cognition. in press

Visscher KM, Kaplan E, Kahana MJ, Sekuler R. Auditory short-term memory behaves like visual short-term memory. PLoS Biology 2007;5(3)

Viswanathan S, Perl DR, Visscher KM, Kahana MJ, Sekuler R. Study list homogeneity and visual short-term recognition. submitted

Wagner A, Shannon B, Kahn I, Buckner R. Parietal lobe contributions to episodic memory retrieval. Trends in Cognitive Science 2005;9 (9):445–453.

Wilson HR, Loffler G, Wilkinson F. Synthetic faces, face cubes, and the geometry of face space. Vision Research 2002;42 (27):2909–2923. [PubMed: 12450502]

Yotsumoto Y, Kahana MJ, Wilson HR, Sekuler R. Recognition memory for realistic synthetic faces. Memory & Cognition Sep;2007 35 (6):1233–1244.

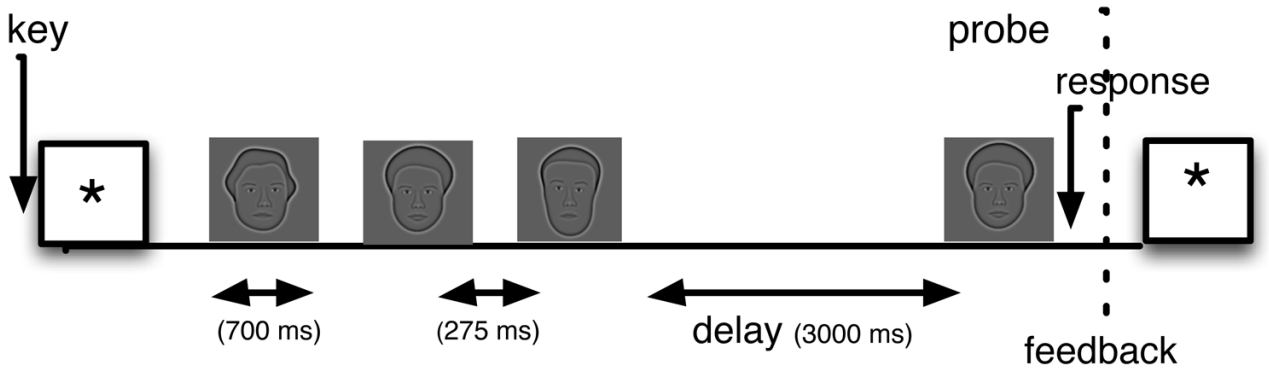

Fig. 1.
Trial structure of the short term item recognition task. Participants see a sequence of 1–3 faces followed by a probe. Their task is to indicate whether the probe matches one of the study items. This figure illustrates a trial with 3 stimuli randomly drawn from a pool of 16 stimuli, as described in the text.

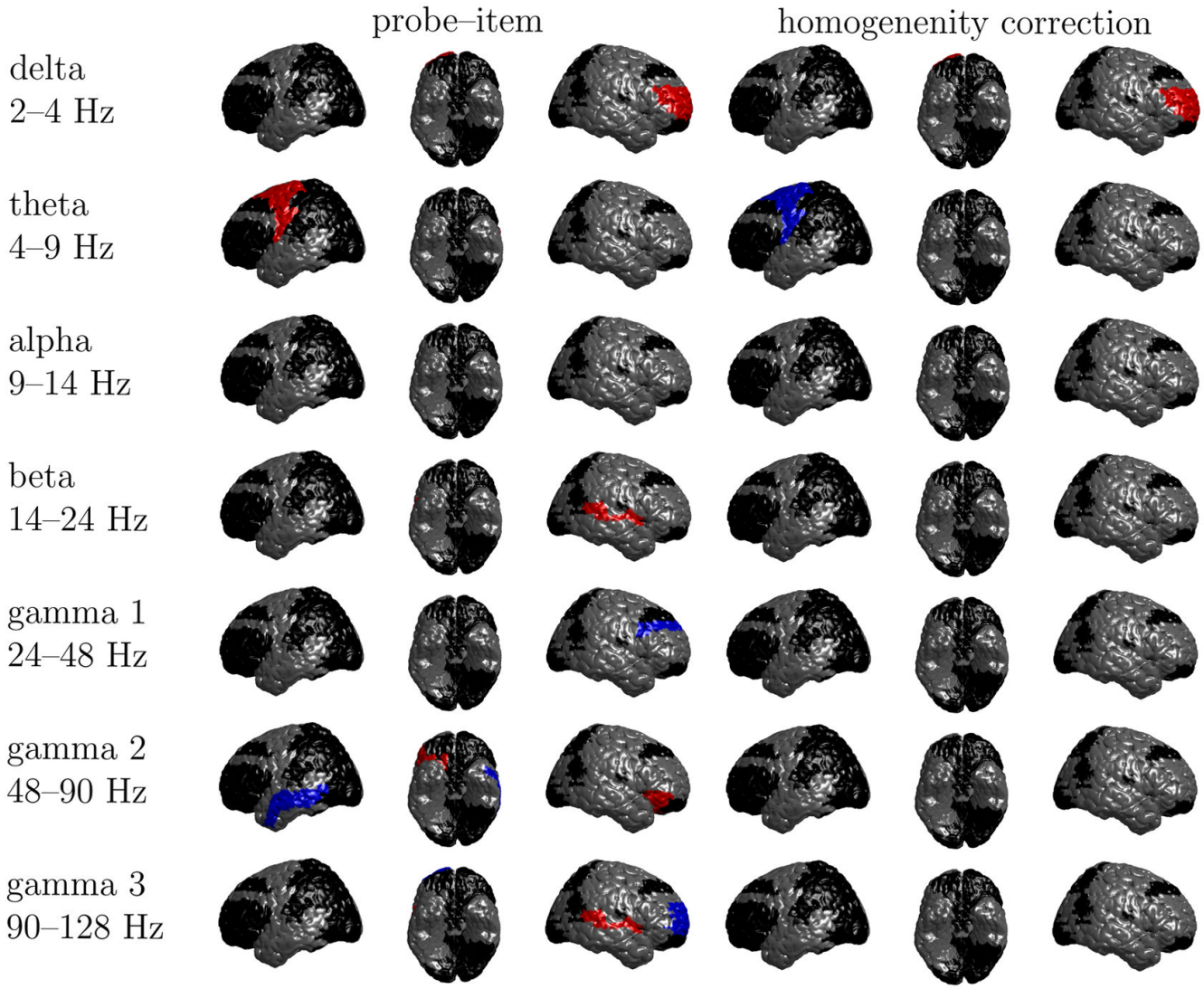

Fig. A.1.

Significant increases (red) and decreases (blue) of oscillatory activity with probe-item similarity and the homogeneity correction for targets. Brodmann areas shown in black do not meet our criterion for doing a statistical analysis. In each row, the views are from left to right: left sagittal, inferior, right sagittal.

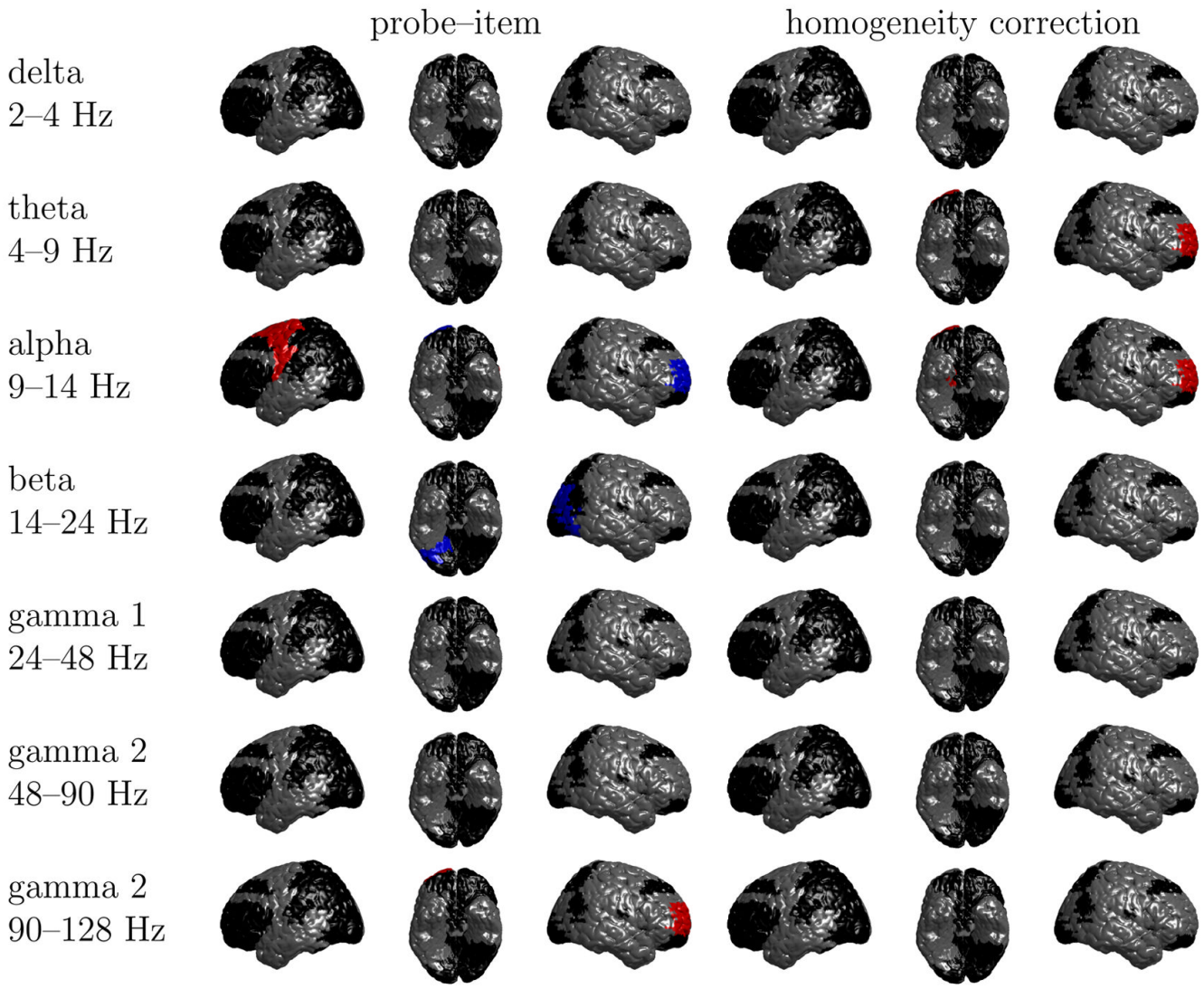

Fig. A.2.
Significant increases (red) and decreases (blue) of oscillatory activity with probe–item similarity and the homogeneity correction for lures. Brodmann areas shown in black do not meet our criterion for doing a statistical analysis. In each row, the views are from left to right: left sagittal, inferior, right sagittal. There is additionally a decrease of 9–14 alpha oscillations with the homogeneity correction in the hippocampus.

Table 1

Modeling short-term recognition of faces: root-mean-square deviation (RMSD) and mean (standard error of mean) NEMo parameters obtained using a genetic algorithm, fitted for each participant separately. Note that α_1 was fixed to 1.

param	faces	param	faces
β	−0.38 (0.13)	τ	8.87 (0.89)
α_2	0.88 (0.021)	c_1	0.35 (0.13)
α_3	0.79 (0.040)	c_2	0.32 (0.15)
α_4	0.68 (0.027)	c_3	0.34 (0.13)
	.	c_4	0.15 (0.36)
σ_1	0.068 (0.053)	w_1	0.088 (0.049)
σ_2	0.078 (0.051)	w_2	0.11 (0.058)
σ_3	0.080 (0.11)	w_3	0.29 (0.092)
σ_4	0.16 (0.039)	w_4	0.50 (0.11)
RMSD	0.168 (0.012)		

Table 2

Overview of significant correlations between probe–item similarity (S) and homogeneity (H) and oscillatory power for lure probes. "l" indicates left hemisphere, whereas "r" indicates right hemisphere. The left column represents probe–item similarity and the right column the homogeneity correction. Frontal areas have a blue background, memory-related areas a yellow background, left parietal areas are pink, and motor areas have a green background. Brodmann areas are considered significant if they show a significant correlation in at least one timebin. The last two columns indicate the number of participants (N_s) and number of electrodes (N_e) in each Brodmann area. For the gamma band, the subscript indicates the gamma sub-band: 1=28–48 Hz; 2=48–90 Hz; 3=90–128 Hz. Abbreviations: BA 10= frontopolar cortex; BA 46: DLPFC; BA 9: DLPFC; BA 21: MTG; BA 22: STG; entorh= entorhinal; hipp=hippocampus; BA 7=parietal; BA 39=parietal; BA 40=parietal; BA 4/6 = (pre-)motor.

Targets

BA	**probe–item similarity**					**homogeneity correction**						
frequency (Hz)	**δ (2–4)**	**θ (4–9)**	**α (9–14)**	**β (14–28)**	**γ (28–128)**	**δ (2–4)**	**θ (4–9)**	**α (9–14)**	**β (14–28)**	**γ (28–128)**	**N_s**	**N_e**
rBA10	S^+				S_3^-	H^+					4	33
rBA46	S^+					H^+					6	13
rBA9					S_1^-						6	20
lBA21					S_2^-						7	52
rBA22				S^+	S_3^+						9	47
r entorh											8	17
r hipp											4	13
lBA7											3	5
lBA39											2	6
lBA40											4	18
lBA4/6		S^+					H^-				4	31

Lures

BA	probe–item similarity					homogeneity correction						
frequency (Hz)	δ (2–4)	θ (4–9)	α (9–14)	β (14–28)	γ (28–128)	δ (2–4)	θ (4–9)	α (9–14)	β (14–28)	γ (28–128)	N_s	N_l
rBA10			S^-		S_3^+		H^+	H^+			4	33
rBA46											6	13
rBA9											6	20
lBA21											7	52
rBA22											9	47
r entorh								H^+			8	17
r hipp								H^+			4	13

Targets												
BA	**probe–item similarity**					**homogeneity correction**						
frequency (Hz)	***δ* (2–4)**	***θ* (4–9)**	***α* (9–14)**	***β* (14–28)**	***γ* (28–128)**	***δ* (2–4)**	***θ* (4–9)**	***α* (9–14)**	***β* (14–28)**	***γ* (28–128)**	N_s	N_e
lBA7											3	5
lBA39											2	6
lBA40											4	18
lBA4/6			S^+								4	31